

⁴ Aggarwal, H. R. and Ablow, C. M., "Solution to a Class of Three-Dimensional Pulse Propagation Problems in an Elastic Half-Space," *International Journal of the Engineering Sciences*, Vol. 5, 1967, pp. 663-679.

⁵ Lord Rayleigh, "On Waves Propagated Along the Plane Surface of an Elastic Solid," *Proceedings of the London Mathematical Society*, Vol. 17, 1885, pp. 4-11.

⁶ Mitra, M., "Disturbance Produced in an Elastic Half-Space by Impulsive Normal Pressure," *Proceedings of the Cambridge Philosophical Society*, Vol. 60, 1964, p. 685.

⁷ Aggarwal, H. R. and Ablow, C. M., "Extension of the Bateman-Pekeris Theorem with Application to a Wave Propagation Problem," *Journal of Mathematics and Physics*, Vol. 44, 1965, pp. 267-270.

⁸ Aggarwal, H. R. and Ablow, C. M., "On the Rayleigh Equation for Elastic Surface Waves," *Journal of the Acoustical Society of America*, Vol. 47, Part 2, 1970, p. 1461.

⁹ Baron, M. L. and Check, R., "Elastic Rayleigh Wave Motions Due to Nuclear Blasts," *Transactions of the ASCE: Journal of the Engineering Mechanics Division*, Vol. 89, No. EM1, 1963, pp. 57-70.

Strongly Coupled Stress Waves in Heterogeneous Plates

A. S. D. WANG,* P. C. CHOU,† AND J. L. ROSE ‡
Drexel University, Philadelphia, Pa.

Introduction

IN the analysis of heterogeneous anisotropic plates,^{1,2} the general equations governing the linear and the rotatory motions of the plate may be expressed by a set of five simultaneous second order partial differential equations. Depending on the heterogeneity and the anisotropy of the plate, strong coupling amongst the displacement functions and their derivatives may exist both in the field equations and in the initial/boundary conditions. A general solution to such a system seems improbable, although a few simplified problems concerning statical or quasi-statical deformations have been solved.

In the present Note, we consider coupled stress waves which are generated by an impulsive load applied on the one end of a semi-infinite plate. The field equations governing the one dimensional coupled waves are readily obtained from the general theory in Refs. 1 or 2. A general form of these equations may be expressed by

$$u_{1,xx} - c_1^{-2}u_{1,t} + A_1u_{2,xx} = R_1 \quad (1a)$$

$$u_{2,xx} - c_2^{-2}u_{2,t} + A_2u_{1,xx} = R_2 \quad (1b)$$

$$u_{3,xx} - c_3^{-2}u_{3,t} = R_3 \quad (1c)$$

where u_i , $i = 1, 2, 3$, denote the generalized displacements; c_i , A_1 , and A_2 may be real, continuous functions of x ; and

$$R_i = \sum_{j=1}^3 (\alpha_{ij}u_j + \beta_{ij}u_{j,x}) \quad i = 1, 2, 3 \quad (2)$$

with α_{ij} and β_{ij} being at most real continuous functions of x .

If in Eq. (1), $A_1 = A_2 = 0$, the system reduces to what is termed as "weakly" coupled hyperbolic system for which a unified solution scheme by the method of characteristics has been presented in Ref. 3. In the present problem however, with $A_1 \neq A_2 \neq 0$, a strong coupling in the second derivatives exists. We shall extend the method described in Ref. 3 and treat the transient

stress waves in a semi-infinite plate, subjected to an initial step input. Coupled discontinuity fronts are found to propagate at different velocities. The normal plate stress and the bending moment at different time regimes are illustrated through graphs.

The Method of Characteristics

Following a similar procedure as outlined in Ref. 3, § the six characteristics of the system of equations (1) are found to be

$$\frac{dx}{dt} = \begin{cases} \pm \{(1+s)/2\}(c_1^2 + c_2^2)^{1/2} = \pm s_1 \\ \pm \{(1-s)/2\}(c_1^2 + c_2^2)^{1/2} = \pm s_2 \\ \pm c_3 \end{cases} \quad (3)$$

where

$$s = \{1 - 4c_1^2c_2^2(1 - A_1A_2)/(c_1^2 + c_2^2)^2\}^{1/2} \quad (4)$$

If all of the six characteristics are real and distinct, the system (1) is said to be totally hyperbolic,⁵ or distinctly hyperbolic.⁶ In what follows, we shall limit our discussions to such a distinctly hyperbolic system. Then, the following inequality must be satisfied everywhere in the physical plane:

$$-(c_1^2 - c_2^2)^2/4c_1^2c_2^2 < A_1A_2 < 1 \quad (5)$$

The six independent equations associated with the six characteristics are given by

$$I_1^\pm: (c_1^2R_1dx - s_1^2du_{1,x} \pm s_1du_{1,t})(c_2^2 - s_1^2) - A_1c_1^2(c_2^2R_2dx - s_1^2du_{2,x} \pm s_1du_{2,t}) = 0 \quad (6)$$

$$I_2^\pm: (c_2^2R_2dx - s_2^2du_{2,x} \pm s_2du_{2,t})(c_1^2 - s_2^2) - A_2c_2^2(c_1^2R_1dx - s_2^2du_{1,x} \pm s_2du_{1,t}) = 0 \quad (7)$$

$$I_3^\pm: R_3dx - du_{3,x} \pm (1/c_3)u_{3,t} = 0 \quad (8)$$

Equations I_1^\pm govern the variables u_i and their first derivatives along, respectively, curves C_1^\pm whose local slopes are respectively $\pm s_1$; similarly, equations I_2^\pm are for curves C_2^\pm whose slopes are $\pm s_2$; and equations I_3^\pm are for curves C_3^\pm with local slopes of respectively $\pm s_3$.

If in a region in the physical plane the first derivatives of u_i are continuous, we have the following additional relations,

$$du_i = u_{i,x}dx + u_{i,t}dt \quad i = 1, 2, 3. \quad (9)$$

The nine equations (6-9) will enable the determination of the nine variables u_i , $u_{i,x}$ and $u_{i,t}$ ($i = 1, 2, 3$), if proper initial and boundary conditions are prescribed. But, when discontinuities in the first derivatives of u_i exist, equations governing their magnitudes must be used in place of Eq. (9). Following a similar but somewhat complicated procedure (for details see Ref. 4) as that outlined in Ref. 3, we can show that discontinuities in the first derivatives of u_i may occur only across a characteristic curve; and for the system of equations (6-8) in particular, discontinuities in $u_{j,x}$ and $u_{j,t}$, ($j = 1, 2$), may occur only across C_j^\pm ; discontinuities in $u_{3,x}$ and $u_{3,t}$ may occur only across C_3^\pm . The equations that govern these discontinuities are given by,

$$[u_{i,x}]_{C_i^\pm} = \mp (1/s_i)[u_{i,t}]_{C_i^\pm} = K_i \exp \{ \int Q_i dx \} \quad i = 1, 2 \quad (10)$$

$$[u_{j,x}]_{C_j^\pm} = \mp (1/s_j)[u_{j,t}]_{C_j^\pm} = [A_j c_j^2 K_j / (c_i^2 - s_j^2)] \exp \{ \int Q_i dx \} \quad i \neq j; \quad i, j = 1, 2 \quad (11)$$

$$[u_{3,x}]_{C_3^\pm} = \mp (1/c_3)[u_{3,t}]_{C_3^\pm} = K_3 \exp \{ \int (\beta_{33}/2) dx \} \quad (12)$$

where

$$Q_i = \frac{A_i \beta_{ji} - (1 - \frac{s_i^2}{c_j^2}) \beta_{ji} + \frac{A_i A_j c_j^2 \beta_{ji}}{c_i^2 - s_j^2} - (1 - \frac{s_i^2}{c_j^2}) \frac{\beta_{ij} A_j c_j^2}{c_i^2 - s_j^2}}{2 \{ s_i^2 A_i A_j / (c_i^2 - s_j^2) - s_i^2 (c_j^2 - s_i^2) / c_i^2 c_j^2 \}} \quad i \neq j; \quad i, j = 1, 2 \quad (13)$$

The notation $[f]_C$ represents the magnitude of discontinuity of the function f across the characteristic curve C . The constants K_i , $i = 1, 2, 3$, must be determined from appropriate initial and

Received November 17, 1971; revision received March 2, 1972. This research is supported in part, by the Air Force Material Laboratory, Non-metallic Division, Wright-Patterson Air Force Base, Ohio; and by NASA through a University Program Grant to Drexel University.

Index categories: Structural Dynamic Analysis; Structural Composite Materials.

* Associate Professor of Applied Mechanics.

† Professor of Aerospace Engineering.

‡ Assistant Professor of Mechanical Engineering.

§ Detail formulations of the characteristic determinant, the characteristic equations, the jump conditions and the numerical procedures are contained in a separate report.⁴

boundary conditions. It is clear from the Eq. (1) that two initial and two boundary conditions are needed for each of the functions u_i . The specification for what is considered as proper initial and boundary conditions is discussed in Ref. 3. Furthermore, in order to avoid too many technicalities, we shall refer the numerical procedures and the details of the computational code developed for the general system discussed here to Refs. 4 and 7. In the following section, we discuss a numerical example.

Coupled Stress Waves in Laminated Plates

We consider a semi-infinite laminated anisotropic plate; the coordinate axis x is to the right, and z is the normal of the plate. At the free end $x = 0$, the plate is subjected to an impulsive loading which is independent of the y axis. According to the theory given and the notations used in Ref. 2, the equations governing the one-dimensional wave motions are

$$A_{11}u_{,xx}^0 + B_{11}\psi_{,xx} = Pu_{,t}^0 + R\psi_{,tt} \quad (14a)$$

$$B_{11}u_{,xx}^0 + D_{11}\psi_{,xx} - kA_{55}(\psi_x + w_{,x}) = I\psi_{,tt} + Ru_{,tt} \quad (14b)$$

$$kA_{55}(\psi_{,x} + w_{,xx}) = Pw_{,tt} \quad (14c)$$

In obtaining these equations the conditions that $v = \psi_y = (\cdot)_{,y} = 0$ were used as it is appropriate to the present problem.

If the density distribution across the plate's thickness is symmetric about the middle plane of the plate, then according to Eq. (13), Ref. 2, $R = 0$. Consequently, the system represented by Eq. (14) identifies with the general system (1), the generalized displacements being $u_1 = u^0$, $u_2 = \psi_x$ and $u_3 = w$.

In addition, the normal plate force N_x and the bending moment M_x are expressed by

$$N_x = A_{11}u_{,x}^0 + B_{11}\psi_{,x}; \quad M_x = B_{11}u_{,x}^0 + D_{11}\psi_{,x,x} \quad (15)$$

For numerical illustration, let us consider a two-layer cross-ply (90°-0°) graphite-epoxy composite plate, having the following properties:

$\rho = 0.0205$ slug/in.³, $\nu_{LT} = 0.25$, $E_T = 10^6$ psi,
 $E_L = 25 \times 10^6$ psi, $G_{LT} = 0.5 \times 10^6$ psi, $G_{TT} = 0.2 \times 10^6$ psi
 where L signifies the property longitudinal to the fiber, T transverse to the fiber. The thickness of the individual ply was taken as 0.005 in., while the shear correction factor k appearing in Eq. (14) was put at $\frac{5}{6}$.

The characteristics of the system are calculated from Eq. (3); and they are $s_1 = 117,100$ in./sec, $s_2 = 39,100$ in./sec, $s_3 = c_3 = 13,060$ in./sec, which insure a distinctly hyperbolic system for the system (1).

The initial and boundary conditions are derived from the assumption that the plate is initially at rest and at $t = 0, x = 0$, a step input of the particle velocity is given for $u_t = 1$ in./sec. Thus a jump in u_t is introduced at the boundary $x = 0$. According to Eqs. (10) and (11), jumps in $u_{,x}$, $\psi_{,t}$, and $\psi_{,x}$ will also occur across both C_1^\pm and C_2^\pm characteristic lines.

To evaluate these jumps, we first note from the stated conditions that

$$[u_{,t}^0]_{x=0} = \{[u_{,t}^0]_{C_1^\pm} + [u_{,t}^0]_{C_2^\pm}\} = 1 \quad (16a)$$

$$[M_x]_{x=0} = \{B_{11}[u_{,x}^0] + D_{11}[\psi_{,x,x}]\}_{x=0} = 0 \quad (16b)$$

For the present problem, $Q_1 = Q_2 = 0$ according to Eq. (13), and from Eqs. (10) and (11) we find

$$[u_{,x}]_{C_1^\pm} = K_1, \quad [\psi_{,x,x}]_{C_2^\pm} = K_2 \quad (17a)$$

$$[\psi_{,x,x}]_{C_1^\pm} = A_2c_2^2K_1/(c_1^2 - s_2^2), \quad [u_{,x}^0]_{C_2^\pm} = A_1c_1^2K_2/(c_2^2 - s_1^2) \quad (17b)$$

Substitution of Eq. (17) into Eq. (16) yields

$$K_1 = -\{1/s_1 + K_2s_2A_1c_1^2/(c_2^2 - s_1^2)\} \quad (18)$$

$$K_2 = \frac{(1/s_1)[B_{11} + D_{11}A_2c_2^2/(c_1^2 - s_2^2)]}{B_{11}\frac{A_1c_1^2}{c_2^2 - s_1^2} + D_{11}\frac{s_2A_1c_1^2}{s_1(c_2^2 - s_1^2)}(B_{11} + D_{11}\frac{A_2c_2^2}{c_1^2 - s_2^2})}$$

Hence the jumps appear to be constant across their respective characteristic curves. It is noted that the present loading con-

dition at $x = 0$ created only two discontinuity fronts, one propagating at the velocity s_1 , the other at s_2 , since no jump is introduced to the w function.[†]

The distribution of M_x and N_x at different times after the initial impact are shown in Figs. 1 and 2. In each case two discontinuity fronts are depicted, propagating at speeds s_1 and s_2 , respectively. It is noted that jumps across each wave front remain constant, although the jumps across the faster front are smaller in magnitude than the corresponding jumps across the slower front. The two fronts separate at a relative speed of $(s_1 - s_2)$ as they propagate.

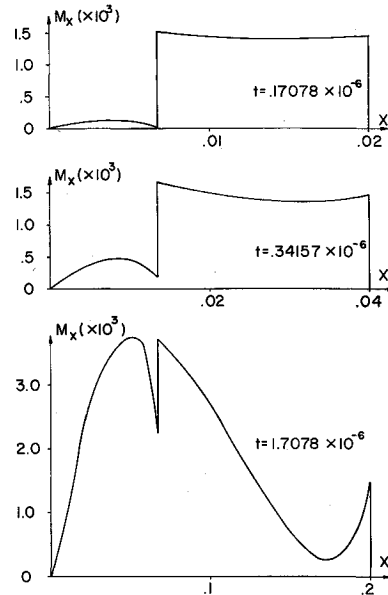


Fig. 1 Moment distribution at three time regimes.

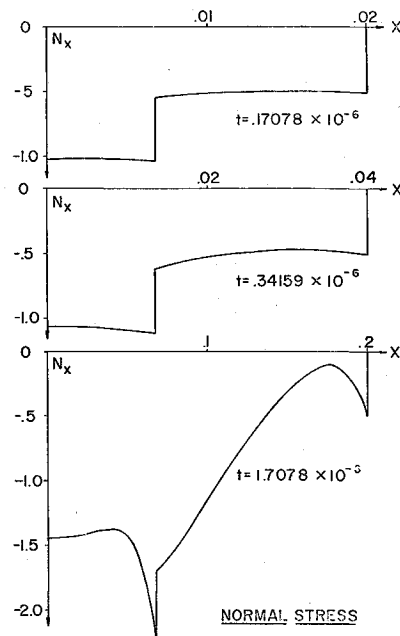


Fig. 2 Normal plate force distribution at three time regimes.

[†]A step input such as $w_{,t} \neq 0$, at $x = 0$, will cause a discontinuity propagating along C_3^\pm at a speed of c_3 .

References

- ¹ Yang, P. C., Norris, C. H., and Stavsky, Y., "Elastic Wave Propagation in Heterogeneous Plates," *International Journal of Solids and Structures*, Vol. 2, 1966, pp. 665-684.
- ² Whitney, J. M. and Pagano, N. J., "Shear Deformation in Heterogeneous Anisotropic Plates," *Journal of Applied Mechanics*, Vol. 37, Dec. 1970, pp. 1031-1036.
- ³ Chou, P. C. and Mortimer, R. W., "Solutions of One-dimensional Elastic Wave Problems By the Method of Characteristics," *Journal of Applied Mechanics*, Vol. 34, Sept. 1967, pp. 745-750.
- ⁴ Wang, A. S. D., Chou, P. C., and Rose, J. L., "On Strongly Coupled Stress Waves in Heterogeneous Plates," TR M & S-71-15, 1971, Drexel Univ., Philadelphia, Pa.
- ⁵ Courant, R. and Hilbert, D., *Methods in Mathematical Physics*, Vol. 2, Wiley, New York, 1962.
- ⁶ Chou, P. C. and Perry, R. F., "The Classification of Partial Differential Equations in Structural Dynamics," Proceedings of AIAA Structural Dynamics and Aero-elasticity Specialists Conference, New Orleans, 1969, pp. 185-194.
- ⁷ Chou, P. C., Hoberg, J. F., and Mortimer, R. W., "MCDU-22, A Computer Code for One-dimensional Elastic Wave Problems Involving Strong Coupling," TR M & S-71,16, 1971, Drexel Univ., Philadelphia, Pa.

Dynamic Snap-Buckling of Shallow Arches under Inclined Loads

V. SUNDARARAJAN* AND D. S. KUMANI†
Indian Institute of Technology, Kanpur, India

Introduction

THE dynamic stability of shallow arches has been studied by many authors (see for example Ref. 1). Most of the works have been concerned with arches under uniformly distributed load. The stability of arches due to static concentrated load acting at the center of the arch is given by Dickie and Broughton.² The dynamic stability of arches subjected to concentrated eccentric load is studied in Refs. 1 and 3. In the present Note the dynamic snap-through of a clamped shallow circular arch by the action of a timewise step concentrated inclined load acting at an arbitrary point is studied. The material of the arch is assumed to be homogeneous, isotropic and linearly elastic.

Formulation and Solution

Referring to Fig. 1, the initial unstressed position of the arch is denoted by $y_0(x)$ and the displacements $w(x, t)$ are measured normal to x axis. Assuming that there is no initial thrust the equation of motion of the shallow arch can be written as

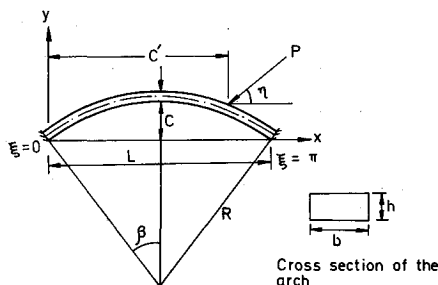


Fig. 1 Geometry of the arch.

Received December 1, 1971; revision received January 24, 1972.
Index categories: Structural Stability Analysis; Structural Dynamic Analysis.

* Associate Professor, Department of Mechanical Engineering.

† Graduate Student, Department of Mechanical Engineering.

$$EI \frac{\partial^4 w}{\partial x^4} - H \frac{\partial^2 (y_0 - w)}{\partial x^2} + \rho A \frac{\partial^2 w}{\partial t^2} + S(x - c')P \cos \eta \frac{\partial^2 (y_0 - w)}{\partial x^2} - P \sin \eta \delta(x - c') = 0 \quad (1)$$

where

$$H = \left(1 - \frac{c'}{L}\right) P \cos \eta + \frac{EA}{2L} \int_0^L \left[\left(\frac{dy_0}{dx}\right)^2 - \left(\frac{dy_0}{dx} - \frac{dw}{dx}\right)^2 \right] dx$$

and

$$S(x - c') = 1 \text{ if } x > c', \quad = 0 \text{ if } x < c'$$

Assuming a circular arch, and introducing nondimensional parameters

$$\phi = w/h, \quad \xi = \pi x/L, \quad \tau = t/R(\bar{E}/\rho)^{1/2}, \quad \gamma = L^2/4hR, \\ \beta = L/2R, \quad e = \pi c/L$$

and

$$F = \pi P L^3 / E b h^4$$

Eq. (1) can be written as

$$\ddot{\phi} + \frac{\pi^4}{192\gamma^2} \phi^{iv} - \left(\phi'' + \frac{4\gamma}{\pi^2}\right) \left\{ \frac{F\pi\beta}{2\gamma} \cos \eta \left(1 - S(\xi - e) - \frac{e}{\pi}\right) - \frac{\pi^3}{32\gamma^2} \left[\int_0^\pi \left\{ \phi'^2 - \frac{8\gamma}{\pi} \left(\frac{1}{2} - \frac{\xi}{\pi}\right) \phi' \right\} d\xi \right] \right\} - F \delta(\xi - e) \sin \eta = 0 \quad (2)$$

where prime denotes $\partial/\partial\xi$ and dot denotes $\partial/\partial\tau$.

Solution is assumed in the form

$$\phi(\xi, \tau) = \sum_{n=1}^{\infty} a_n(\tau) \phi_n(\xi) \quad (3)$$

where $\phi_n(\xi)$ are the eigenfunctions for normal modes of vibration of a clamped flat beam with corresponding eigenvalues m_n . Substituting Eq. (3) in Eq. (1), multiplying by ϕ_s , integrating from 0 to π and making use of the orthogonal property of ϕ_n , the following equations are obtained:

$$\ddot{a}_s + \frac{(m_s \pi)^4}{192\gamma^2} a_s + \frac{1}{A_s} \left(B_s + \frac{\pi^2}{4\gamma} \sum_{n=1}^{\infty} a_n D_{sn} \right) \times \\ \left(\frac{\pi}{8\gamma} \sum_{m=1}^{\infty} \sum_{n=1}^{\infty} a_m a_n D_{mn} + \frac{B_s}{\pi} \sum_{n=1}^{\infty} a_n \right) + \frac{2F\beta \cos \eta}{\pi A_s} \times \\ \left[\left(C_s - \frac{e}{\pi} B_s \right) + \frac{\pi^2}{4\gamma} \sum_{n=1}^{\infty} a_n \left(G_{sn} - \frac{e}{\pi} D_{sn} \right) \right] - \frac{F \sin \eta}{A_s} H_s = 0 \quad (4)$$

Where A_s , B_s , C_s , D_{sn} , G_{sn} are definite integrals involving the eigenfunctions ϕ_n and $H_s = \phi_s|_{\xi=e}$. The amplitude $a_s(\tau)$ of the response can be calculated for different loads from the above sets of equations.

The critical snap buckling load is defined as that load for which a small increase in load produces a large increase in deflection. To arrive at this buckling load an average deflection ratio Δ defined as follows is introduced⁴:

$$\Delta(t) = \frac{1}{L} \int_0^L w(x, t) dx / \frac{1}{L} \int_0^L y_0(x) dx$$

and a value of Δ greater than unity indicates large deflection.

Numerical results and discussion

Equation (4) was integrated numerically using an IBM 7044 digital computer for a specified load (F), position of the load (e), inclination of the load (η), and maximum arch rise ($k = c/2h$) considering the first four terms in Eq. (3). The average deflection ratio (Δ) is calculated at different time τ . The load F and the time τ at which Δ becomes greater than 1 represents the buckling load and the time at which snap-through occurs.

The variation of the snap-through load with the maximum arch rise when $\eta = 30^\circ$ is shown in Fig. 2. The snap-through load for different positions of the load for an arch rise $k = 3$ is plotted in Fig. 3. The effect of the inclination of the load also is shown. In the case when $\eta = 90^\circ$ the snap load is symmetrical about the